Nucl. Sci. and Tech., Vol.10, No. 4 (2020), pp. 01-07

Nuclear Science and Technology

Journal homepage: https://jnst.vn/index.php/nst

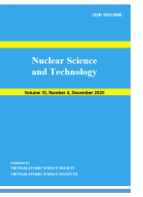

Simulation of absorbed doses distribution in a polyethylene phantom for BNCT application at the Dalat research reactor

Pham Dang Quyet[1*], Pham Ngoc Son[2], Nguyen Nhi Dien[2], Nguyen An Son[1], Trinh Thi Tu Anh[1], Cao Dong Vu[2]

[1]The University of Dalat, 01 Phu Dong Thien Vuong Street, Dalat, Lamdong
[2]Nuclear Research Institute, 01 Nguyen Tu Luc Street, Dalat, Lamdong
**Email: quyetpd@dlu.edu.vn*

Abstract: In this paper, the distribution of absorbed dose components in a polyethylene phantom for BNCT application at Dalat Nuclear Research Reactor (DNRR) were calculated using the MCNP5 code. The configuration of horizontal neutron channel No.2 of the DNRR, which contains a cylindrical collimator with neutron filters of 20-cm Si and 3-cm Bi, was simulated. The results show that the gamma dose along the central axis of the phantom has the maximum value of 1.82×10^{-6} Gy at the 0.5-cm depth, and reduces to 9.05×10^{-7} Gy at the 3-cm depth. The main contribution to gamma dose is due to the interaction of thermal neutron with hydrogen in the phantom via the $^{1}H(n,\gamma)^{2}H$ reaction, and its value is much smaller than thermal neutron dose. The total absorbed dose along the central axis of the phantom has the maximum value of 7.87×10^{-5} Gy at the 0.5-cm depth, and decreases rapidly to 1.52×10^{-5} Gy at the 3-cm position, and mainly depends on the boron and thermal neutron doses caused by the $^{10}B(n, \alpha)^{7}Li$ and $^{14}N(n, p)^{14}C$ reactions, respectively.

Keywords: *Dose distribution, BNCT, polyethylene phantom, thermal neutron flux.*

I. INTRODUCTION

Boron neutron capture therapy (BNCT) is an effective cancer treatment method for several types of brain tumors such as Glioblastoma Multiforme (GBM), Astrocytomas, etc. This method is based on the nuclear reaction that occurs when a stable isotope, ^{10}B, is irradiated with thermal neutrons (with the energy < 0.05 eV) to produce high linear transfer (LET) ^{4}He nuclei (α-particles) and ^{7}Li recoiling nuclei [1, 2].

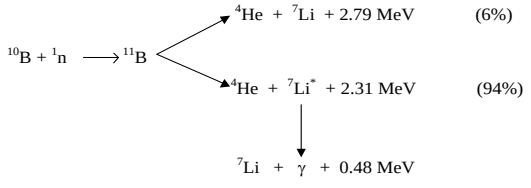

As it is seen, in 94% of the events the released energy of 2.31 MeV of two above particles is deposited within about a cell diameter (~ 10 μm) and the rest i.e. 0.48 MeV is deposited by the emitted gamma ray throughout the medium. Because the high LET of two particles (^{4}He ~ 150 keV/μm and ^{7}Li ~ 175 keV/μm) have limited path lengths in tissue (5 ÷ 9 μm) [1, 3], therefore, it can selectively destroy tumor cells and spare normal cells [4].

Up to now, the best neutron source for BNCT is a thermal nuclear research reactor [3]. In some reactors, such as HANARO in the Republic of Korea [5] and MURR in the USA [6], the single crystal filters of Si and Bi are used to produce thermal neutrons for BNCT research. The in-phantom depth absorbed dose

https://doi.org/10.53747/jnst.v10i4.9
Received 26 November 2020, accepted 28 December 2020

distribution for BNCT application has been computed using the MCNP5 code [7-9]. In case of the TRR and MNSR reactors in Iran, the absorbed doses distribution in phantoms were computed based on the thermal column of the reactor, however gamma-rays dose that include gamma rays from reactor and captured gamma rays in material of the phantom were not estimated [8-9]. Two types of materials, which are usually used for designing a phantom for BNCT research, are water and polyethylene because their densities are similar to that of a tissue. Polyethylene phantoms have been used for experimental trial at the LVR-15 reactor in Czech Republic, the KUR reactor in Japan, and the BMRR reactor in USA [10]. Water phantoms have been used experimentally at the JRR No. 4 in Japan [11], the TRIGA Puspati reactor in Malaysia [12] and the TRR reactor in Iran [13]. The prototype water phantom was also developed for the design simulation of thermal neutron collimators for neutron capture studies at the DNRR [14]. The purpose of this study is to simulate the distribution of absorbed dose components in the polyethylene phantom for BNCT research. The recent configuration of the horizontal neutron channel No.2 of the DNRR were simulated using the MCNP5 code. The absorbed doses distribution in the polyethylene phantom at the horizontal channel No.2 was then calculated.

II. MATERIALS AND METHODS

The DNRR is a 500-kW pool-type research reactor, which was reconstructed and upgraded from the former 250-kW TRIGA Mark II reactor. Light water is used as both moderator and coolant, and the beryllium and graphite materials surrounding the reactor core are used as a neutron reflector. The operation of the DNRR is mainly for the purposes of radioisotope production, neutron activation analysis, basic and applied research, and training [15].

The reactor has four horizontal neutron channels that penetrate the concrete shield and the aluminum tank and pass through the pool water to the graphite reflector. Three of the neutron channels (No.1, No.2 and No.4) are oriented radially with respect to the center of the reactor core, and the channel No.3 is tangential to the outer edge of the reactor core. The radial channel No.2 terminates at the outer edge of the graphite reflector that can produce a relatively high thermal neutron flux. This is the reason that the neutron channel No.2 was chosen in this study. The configuration of the horizontal channel No.2 of the DNRR is presented in Fig. 1.

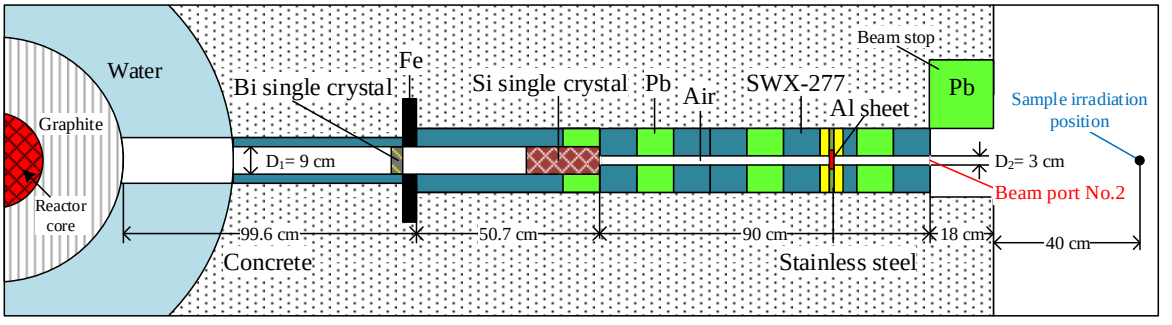

Fig. 1. The configuration of the horizontal channel No.2 of the DNRR

As seen in Fig. 1, after traversing the filters including Si and Bi single crystal layers, with the thicknesses of 20 and 3 cm, respectively, thermal neutron beam will be produced for different applications, including nuclear data measurement, prompt gamma neutron activation analysis (PGNNA) and BNCT study [16]. The simulated and measured thermal neutron fluxes and gamma dose rates at 1-cm depth in the water phantom at the channel No.2 are shown in Table I [14]. Then, the simulated results have been normalized according to the experimental values to calculate thermal neutron flux and gamma dose rate distributions in the polyethylene phantom.

Table I. Simulated and measured results of the thermal neutron flux and gamma dose rate in the water phantom at the channel No.2

Parameters	Simulation	Experimental
Thermal neutron flux ($n/cm^2/s$)	2.27×10^{7}	$(2.13 \pm 0.04)\times10^{7}$
Gamma dose rate (Gy/h)	3.33×10^{-3}	$(3.01 \pm 0.90)\times10^{-3}$

In this study, the polyethylene phantom (ρ = 0,92 g/cm^3) with its length, width and depth of 25, 16 and 16 cm, respectively, was used and located at 40 cm far from the beam port of the channel No.2 (Fig. 2).

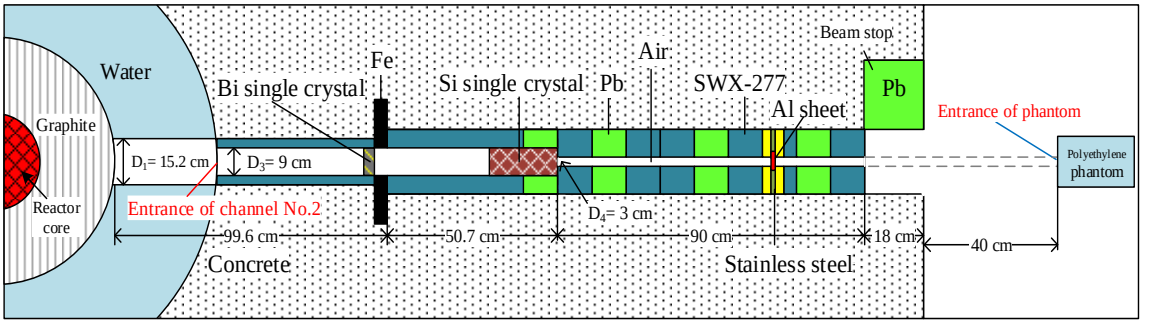

Fig. 2. The real phantom position at the channel No.2 of the DNRR

In BNCT, there are four components of interested absorbed dose: the boron dose, the thermal neutron dose, the gamma dose, and the fast neutron dose. However, for the current configuration of channel No.2, the fast neutron dose is very low and can be eliminated [14], so the total absorbed dose in BNCT is calculated by equation [8]:

$$D = D_B + D_N + D_\gamma \quad (1)$$

Where, D is the total absorbed dose, D_B is the boron dose, D_N is the thermal neutron dose, and $D\gamma$ is the gamma dose that includes gamma from the reactor core and gamma due to interaction of thermal neutron with the hydrogen of phantom by the $^1H(n,\gamma)^2H$ reaction. The D_B and D_N doses are determined as [17]:

$$D_B = 7.43 C_B \times 10^{-14} \times \Phi_{th} \quad (2)$$

and

$$D_N = 6.78 C_N \times 10^{-14} \times \Phi_{th} \quad (3)$$

In which, C_B is the ^{10}B concentration (the value in this calculation was chosen of 30 ppm [1, 7]), C_N is the ^{14}N concentration (it was chosen of 2 % [17]), and Φ_{th} is the thermal neutron fluence (n/cm^2). In BNCT, when calculating the dose, the concept of thermal neutron fluence (Φ_{th}) is used instead of the thermal neutron flux (ϕ_{th}). The relationship between these two quantities is calculated as follows:

$$\Phi_{th} = \phi_{th} \times t \quad (4)$$

Where, ϕ_{th} is the thermal neutron flux (n/cm^2/s), and t is time (s).

The thermal neutron flux and gamma dose rate in the polyethylene phantom were calculated using tally F4 with DE4/DF4 cards of MCNP5, the gamma dose was determined using the fluence-to-KERMA conversion factors reported in ICRU 63 [18]. With these MCNP cards we can calculate the following values of thermal neutron flux and the gamma dose rate [8, 9]:

$$\phi_{th} = \int_{E_1}^{E_2} \varphi_n(E)dE \quad (5)$$

$$\dot{D}_\gamma = \int_{E_1}^{E_2} \varphi_n(E)R(E)dE \quad (6)$$

Where, ϕ_{th} is the thermal neutron flux, $\varphi_n(E)$ is the neutron flux, E_1 and E_2 are the lower and upper limit of the energy range, respectively, $\dot{D}_\gamma$ is the gamma dose rate and R(E) is the flux to dose conversion factor.

III. RESULTS AND DISCUSSION

The thermal neutron flux and gamma dose distributions along the central axis of the polyethylene phantom at the neutron horizontal channel No.2 were calculated and the results are shown in Tables II and III, respectively.

Table II. The thermal neutron flux along central axis of the polyethylene phantom

No.	Position (cm)	ϕ_{th} (n/cm^2/s)		No.	Position (cm)	ϕ_{th} (n/cm^2/s)	
	z	Mean	Err. (%)		z	Mean	Err. (%)
1	0	2.91×10^7	1.0	7	5	1.89×10^6	4.3
2	0.5	3.33×10^7	1.2	8	6	1.18×10^6	5.1
3	1	2.43×10^7	1.4	9	7	7.12×10^5	7.2
4	2	1.24×10^7	2.0	10	8	4.65×10^5	8.0
5	3	6.41×10^6	2.6	11	9	2.88×10^5	8.5
6	4	3.60×10^6	3.4	12	10	1.78×10^5	12.5

Table II and Fig. 3 show that the thermal neutron flux has the maximum value of 3.33×10^7 n/cm^2/s at 0.5-cm depth and then decreases to 6.41×10^6 n/cm^2/s at 3-cm depth in the polyethylene phantom.

Table III. The gamma dose along central axis of the polyethylene phantom

No.	Position (cm) z	D_γ (Gy) Mean from reactor with phantom	Err. (%)	D_γ (Gy) Mean from reactor without phantom	Err. (%)
1	0	1.18×10^{-6}	4.5	4.06×10^{-9}	17.2
2	0.5	1.82×10^{-6}	4.6	5.28×10^{-9}	25.7
3	1	1.69×10^{-6}	5.0	4.24×10^{-9}	17.1
4	2	1.18×10^{-6}	5.3	4.16×10^{-9}	17.1
5	3	9.05×10^{-7}	6.0	4.94×10^{-9}	18.1
6	4	5.61×10^{-7}	7.1	4.14×10^{-9}	17.4
7	5	3.87×10^{-7}	7.2	4.82×10^{-9}	17.8
8	6	2.93×10^{-7}	9.0	5.29×10^{-9}	18.9
9	7	2.26×10^{-7}	7.9	4.62×10^{-9}	17.6
10	8	2.15×10^{-7}	20.0	4.36×10^{-9}	20.2
11	9	1.43×10^{-7}	9.3	3.87×10^{-9}	17.8
12	10	9.52×10^{-8}	11.0	3.33×10^{-9}	18.1

As can be seen in Table III and Fig. 4, the gamma dose in the polyethylene phantom is dominated by gamma rays produced by the thermal neutron capture reactions. At the surface of the phantom, gamma dose increases from 4.06×10^{-9} Gy (without the phantom) to 1.18×10^{-6} Gy (with the phantom). The gamma dose in the phantom arises due to the thermal neutron capture reaction as $^1H(n,\gamma)^2H$.

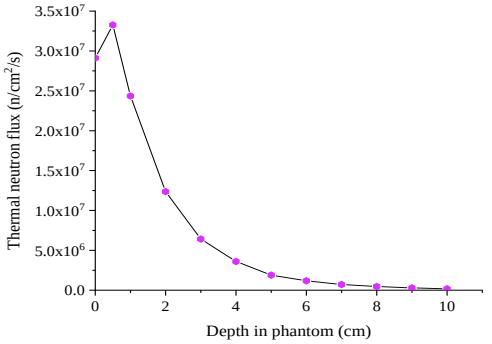

Fig. 3. Thermal neutron flux distribution according to the phantom depth

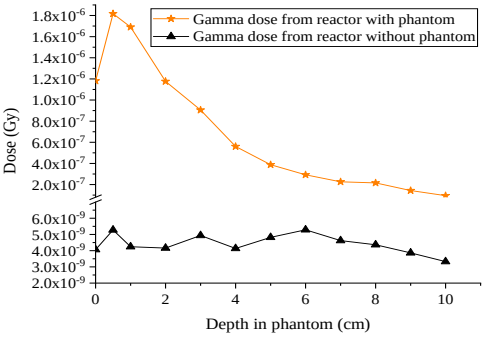

Fig. 4. Gamma doses distribution according to the phantom depth

Figs. 3 and 4 show that the thermal neutron flux and the gamma dose curves have the same shape. The reason is that the gamma dose mixed in the incident neutron beam from the reactor core is relatively low. It means that the gamma dose is mainly dominated by the thermal neutron capture reaction as $^1H(n,\gamma)^2H$.

MCNP5 calculations have shown that the thermal neutron dose is much higher than the gamma dose (Fig. 5), which is the difference of BNCT applications that are based on the horizontal neutron channel in comparison to the thermal column of a nuclear reactor. In Fig. 6, the absorbed

doses along the central axis of the polyethylene phantom are presented. The total absorbed dose mainly due to the contribution of the boron and thermal neutron doses, and it has the maximum value of 7.87×10^{-5} Gy at the 0.5-cm depth and decreases rapidly to 1.52×10^{-5} Gy at the 3-cm depth in the phantom.

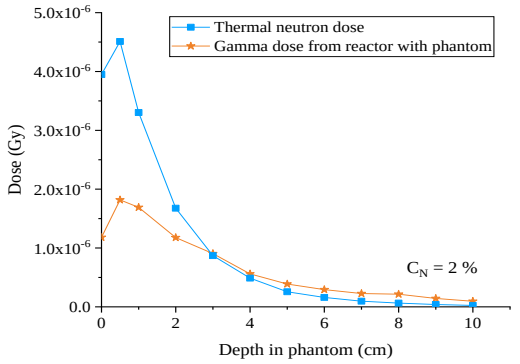

Fig. 5. Gamma and thermal neutron dose distribution according to the phantom depth

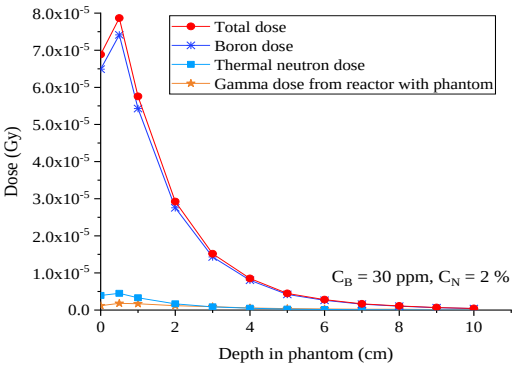

Fig. 6. Distribution of all absorbed doses according to phantom depth

IV. CONCLUSIONS

Calculations of thermal neutron flux and gamma dose rate in the polyethylene phantom were performed to evaluate the absorbed dose components in BNCT application. Calculated absorbed dose distribution along the central axis of the polyethylene phantom shows that the total absorbed dose has the maximum value of 7.87×10^{-5} Gy at the 0.5-cm depth in the phantom, and is mainly dependent on the boron and thermal neutron doses with the dominant component of boron dose. Maximum thermal neutron flux at the 0.5-cm depth in the phantom is 3.33×10^{7} n/cm^2/s^1.

REFERENCES

[1]. Barth R. F., Soloway A. H. and Fairchild R. G., “Boron Neutron Capture Therapy of Cancer”, Cancer Research, 50, pp. 1061-1070, 1990.

[2]. Barth R. F., Vicente M. G. H., Harling O. K. et al., “Current status of boron neutron capture therapy of high grade gliomas and recurrent head and neck cancer”, Radiation Oncology, 7, pp. 146, 2012.

[3]. Matsumoto T., “Design of neutron beams for boron neutron capture therapy for Triga reactor”, Journal of Nuclear Science and Technology, 33 (2), pp.171-178, 1996.

[4]. Barth R. F., Coderre J. A., Vicente M. G. H. and Blue T. E., Boron Neutron Capture Therapy, Current Status and Future Prospects, pp. 431-459, 2005.

[5]. Myong-Seop K., Byung-Chul L., Sung-Yul H. et al., “Development and characteristics of the HANARO neutron irradiation facility for applications in the boron neutron capture therapy field”, Phys. Med. Biol., 52, pp. 2553-2566, 2007.

[6]. Brockman J., Nigg D. W., Hawthorne M. F. and McKibben C., “Spectral performance of a composite single-crystal filtered thermal neutron beam for BNCT research at the University of Missouri”, Applied Radiation and Isotopes, 67, pp. 223-225, 2009.

[7]. Nigg D. W. and Eng D., “Methods for radiation dose distribution analysis and treatment planning in boron neutron capture therapy”,

Int. J. Radiat. Oncol. Biol. Phys., 28(5), pp. 1121-1134, 1994.

[8]. Kasesaz Y., Bavarnegin E., Golshanian M. et al., "BNCT project at Tehran Research Reactor: current and prospective plans", Progress in Nuclear Energy, 91, pp. 107, 2016.

[9]. Monshizadeh M., Kasesaz Y., Khalafi H. and Hamidi S., "MCNP design of thermal and epithermal neutron beam for BNCT at the Isfahan MNSR", Progress in Nuclear Energy, 83, pp. 427-432, 2015.

[10]. Allen B. J, Moore D. E. and Harrington B. V., Progress in neutron capture therapy for cancer, New York, 1992.

[11]. Yamamoto T., Matsumura A., Yamamoto K., Kumada H., Shibata Y. and Nose T., "In-phantom two-dimensional thermal neutron distribution for intraoperative boron neutron capture therapy of brain tumours", Phys. Med. Biol. 47, pp. 2387–2396, 2002.

[12]. Solleh M. R. M., Mohamed A. A., Tajuddin A.A., Rabir M. H., Zin M. R. M., Yazid H., Azman A., Yoshiaki K. and Hiraga F., Neutron and gamma measurement with water phantom for boron neutron capture therapy (BNCT) reactor Triga Puspati, 2014.

[13]. Bavarnegin E., Sadremomtaz A., Khalafi H. and Kasesaz Y., "Measurement of in-phantom neutron flux and gamma dose in Tehran research reactor boron neutron capture therapy beam line", J. Canc. Res. Therapy, 12(2), 2016.

[14]. Pham Dang Quyet, Pham Ngoc Son, Nguyen Nhi Dien, Trinh Thi Tu Anh and Cao Dong Vu, "Simulation design of thermal neutron collimators for neutron capture studies at the Dalat Research Reactor", Asian Journal of Scientific Research, 13(3), pp. 214-218, 2020.

[15]. Nguyen Nhi Dien et al., Utilisation of the Dalat Research Reactor after its core conversion, Joint IGORR 2014/ IAEA Technical Meeting, 17–21 November, Bariloche, Argentina, 2014.

[16]. Pham Ngoc Son, Vuong Huu Tan, Nguyen Nhi Dien, Nguyen Xuan Hai, Tran Tuan Anh, Ho Huu Thang and Cao Dong Vu, "Development of thermal filtered neutron beam based on the radial channel No. 2 of Dalat research reactor", The Annual Report for 2010, Science and Technics Publishing House, pp. 21-27, 2010.

[17]. Nakagawa Y., Pooh K., Kobayashi T. et al., "Clinical review of the Japanese experience with boron neutron capture therapy and a proposed strategy using epithermal neutron beams", J. Neuro-Oncol., 62, pp. 87-99, 2003.

[18]. Masouli S. F., "Simulation of the BNCT of brain tumors using MCNP code: beam designing and dose", Iran J. Med. Phys., 9 (3), 2012.